On the vertical plasma drift conditions prior to post-midnight ESF

Alexander A. Massoud[1,*], Fabiano S. Rodrigues[1], Karim M. Kuyeng[2], and Danny E. Scipión[2]
1. The University of Texas at Dallas, William B. Hanson Center for Space Sciences, Richardson, TX, USA
2. Instituto Geofísico del Perú, Radio Observatorio de Jicamarca, Lima, Peru
EQIT-5
*Alexander.Massoud@UTDallas.edu

1. INTRODUCTION AND MOTIVATION

Introduction

- Equatorial spread F (ESF) is the general name given to ionospheric F-region irregularities observed at equatorial and low latitudes.
- Typical pre-midnight ESF is commonly attributed to upward vertical plasma drifts associated with the pre-reversal enhancement (PRE) around sunset hours [Fejer et al., 1999].
- Atypical ESF observed outside the ESF season and/or during post-midnight hours is subject to ongoing study [Huba, 2023].
- Progress in understanding post-midnight ESF has been limited in part by (1) difficulties in determining when and where ESF originates and (2) limited availability of equatorial drift measurements.

Motivation

- AMISR-14 is an ultra-high frequency (UHF) radar system at the Jicamarca Radio Observatory (JRO) that can create two-dimensional (2D) "scans" of F-region ESF over a relatively wide field of view (~400 km in the zonal direction) [Rodrigues et al., 2023].
- The medium power mode of the Jicamarca ISR (MP ISR) is a new capability of the Jicamarca radar that has now been producing semi-routine measurements of equatorial drifts [Kuyeng et al., 2023].

➢ **Here, we present analyses of AMISR-14 and Jicamarca MP ISR observations that address the equatorial vertical drift conditions preceding post-midnight ESF.**

2. RELEVANCE

- In this presentation, we highlight that a better understanding of the conditions leading to ESF development requires collocated measurements of ionosphere-thermosphere (IT) parameters at the location where ESF originates.
- This has been a difficult task since most instruments detect ESF signatures without information about the location of its origin. Also, in most cases, ESF measurements are not accompanied by measurements of IT parameters.

➢ **The analysis presented here expands upon previous efforts by using 2D AMISR-14 observations to identify events that developed locally, that is, within ~200 km zonal distance of the JRO. Then, the Jicamarca ISR can reveal the ionospheric conditions under which these events develop.**

- In the case of post-midnight ESF, it has been invoked that abnormal upward drifts can create conditions leading to ESF development [e.g., Yizengaw et al., 2013].

➢ **Here, our results utilize new instrumentation to provide unprecedented observations of the drift conditions leading to post-midnight ESF.**

3. SCIENCE QUESTIONS

- **SQ1.** What are the local vertical plasma drift conditions preceding the development of ESF over Jicamarca?
- **SQ2.** Through what mechanism(s) may atypical nighttime vertical drifts develop and then contribute toward the generation of post-midnight ESF?

4. ANALYSIS

- New 2D observations of ESF started to be made semi-routinely in July 2021 by AMISR-14, a 14-panel version of an AMISR system, installed at the JRO [Rodrigues et al., 2023].
- AMISR-14 uses a 10-beam radar mode to create "images" of the distribution of irregularities in the equatorial F-region plane near Jicamarca.
- **Figure 1** shows an example of measurements made by AMISR-14. The top panel shows the Range-Time-Intensity (RTI) map for echoes observed by the beam closest to zenith. Each bottom panel shows the 2D distribution of UHF echoes constructed with observations made by the 10 beams. The 2D images can show the distribution of ESF echoes within ~200 km of JRO.
- The sequence of 2D images illustrate the detection of a post-midnight ESF plume that developed to the west of JRO before moving into the AMISR-14 field of view.

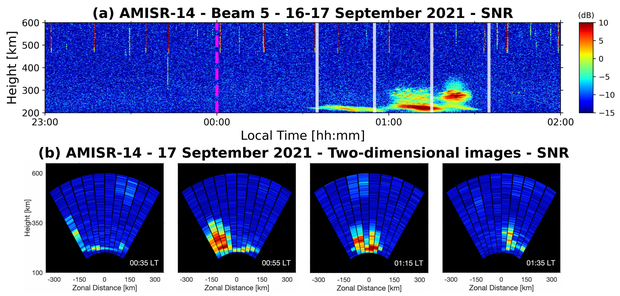

Figure 1. RTI map of UHF coherent echoes measured by AMISR-14 beam 5 (i.e., near zenith) between 23:00 LT on 16 Sep. and 02:00 LT on 17 Sep. 2021 (top panel). Local midnight is indicated by the dashed magenta line. Transparent white solid lines mark the time of each snapshot. Sequence of AMISR-14 2D images (bottom panels). Snapshot timestamps are also indicated in each panel.

- As part of the present study, we analyzed 396 nights of AMISR-14 2D observations between July 2021 and August 2023.
- We identified 51 cases of "isolated" post-midnight ESF events.
- Isolated post-midnight ESF events were F-region echoes seen in the beam near zenith RTI map that appeared in the post-midnight sector after at least 1 hour without any echoes.
- We then inspected 2D images of the 51 isolated post-midnight ESF events to determine whether the events were generated locally, that is, within the AMISR-14 field-of-view (i.e., within ~200 km zonal distance of the JRO at F-region heights).
- **Table 1** shows the event statistics organized by year and season.

Table 1 – Number of observations analyzed and number of local/non-local isolated post-midnight ESF events organized by year and season (Values for quiet time in parentheses).

	2021			2022			2023		
Season	No. of obs.	No. of local events	No. of non-local events	No. of obs.	No. of local events	No. of non-local events	No. of obs.	No. of local events	No. of non-local events
Mar. equ.	-	-	-	56 (20)	4 (1)	2 (0)	40 (11)	0 (0)	1 (0)
Jun. sols.	18 (11)	2 (1)	4 (2)	24 (14)	3 (1)	2 (1)	40 (14)	1 (0)	2 (0)
Sep. equ.	43 (30)	5 (2)	3 (1)	65 (21)	3 (1)	3 (0)	-	-	-
Dec. sols.	51 (27)	6 (3)	4 (3)	59 (24)	3 (2)	3 (2)	-	-	-

➢ **As a result of our analyses of AMISR-14 measurements, we found that ~50% (27 out of 51) of the isolated post-midnight events were generated locally.**

➢ **We also found that 16 of the 27 local ESF events (~60%) occurred during geomagnetically disturbed conditions (Kp >= 3 any time during observation or 12 hours prior to 18:00 LT).**

5. RESULTS AND DISCUSSION

- We now present and discuss observations of a local isolated post-midnight ESF event detected by AMISR-14 on the night of 31 May-1 June 2023 when collocated drift measurements made by the Jicamarca MP ISR mode were also available.

5.1. ON THE DRIFTS PRIOR TO POST-MIDNIGHT ESF

- **Figure 2** summarizes MP ISR and AMISR-14 observations made on the night of 31 May-1 June 2023.
- **Figure 2a** shows the RTI map of the echoes observed by the MP ISR. It shows the occurrence of a bottom-type layer in the pre-midnight sector and an isolated topside ESF event in the post-midnight sector.
- **Figure 2b** shows the drift measurements made by the MP ISR. Drifts at heights and local times with ISR echoes that were too weak or affected by ESF echoes were not reported or shown.
- **Figure 2c** shows height-averaged F-region drifts measured by the MP ISR. For reference, it also shows the prediction of quiet-time drifts by the Scherliess and Fejer (1999) empirical model (SF99).
- Finally, **Figure 2d** shows a sequence of AMISR-14 2D images for the period between 04:55 LT and 05:25 LT that illustrates the local development of the post-midnight ESF event.

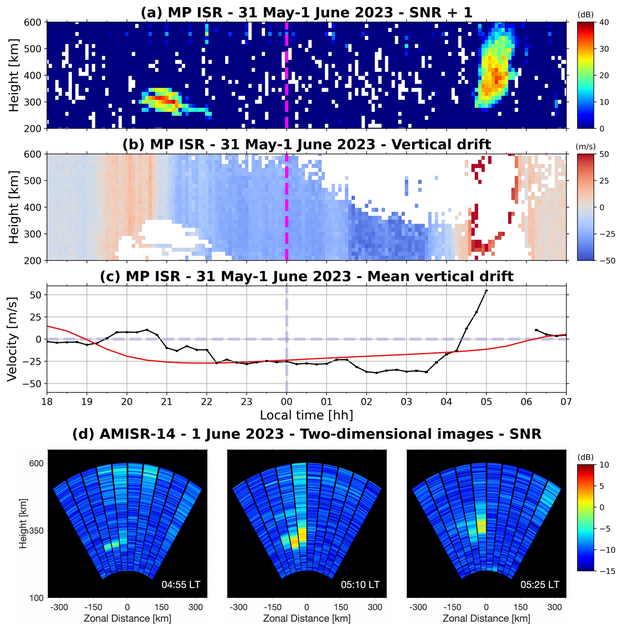

Figure 2. RTI map of MP ISR coherent echoes (panel a), vertical drifts (panel b), and mean vertical drifts (panel c). Sequence of AMISR-14 2D images (panel d).

- Of relevance to this study is the collocated observations of ESF and drift conditions. Figure 4c shows that the drifts deviated significantly from SF99 quiet-time expectations.
- First, during the evening of May 31, a weak PRE was measured around 20:00 LT.
- Most importantly, drifts changed dramatically starting around 03:30 LT when they were strongly downward (~-35 m/s). By 04:45 LT, before the ESF event occurred, the drifts were upward and reached magnitude greater than 25 m/s.

➢ **The collocated 2D observations by AMISR-14 and the MP ISR allowed us to examine, unambiguously, the vertical drift conditions preceding a post-midnight ESF event that developed over Jicamarca. These collocated observations provide experimental evidence supporting the suggestion of abnormal upward drifts creating conditions conducive to the generation of post-midnight ESF [Zhan et al., 2018](SQ1).**

➢ **The upward drifts would create conditions favoring the development of ESF by contributing directly to the linear growth rate of the Generalized Rayleigh Taylor (GRT) instability, which is commonly invoked to explain the development of spread-F at equatorial and low latitudes [Sultan, 1996] (SQ2).**

5.2. ON THE SOURCE OF UPWARD DRIFTS

- **Figure 3** describes the geomagnetic conditions between 30 May and 3 June 2023 through the SYM-H, auroral electrojet (AE), and Planetary K (Kp) indices. The red transparent line marks the period when post-midnight ESF was observed.

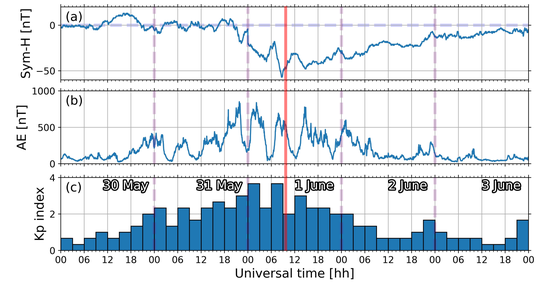

Figure 3. Geomagnetic indices for the period of interest: (a) SYM-H, (b) AE, and (c) Kp.

- Figure 3 shows the June 1st event occurred during geomagnetically disturbed conditions associated in our analyses with Kp >= 3 at any point during the nighttime AMISR-14 observations or 12 hours prior.
- The SYM-H index shows a sudden storm commencement (SSC) around 20:00 UT (~15:00 LT) on May 31. The main phase of the storm lasted until about 08:30 UT (03:30 LT) on June 1 when SYM-H reached its minimum value (~ -55 nT).

➢ **Based on SYM-H, the storm can be classified as one of moderate intensity [Gonzalez et al., 1994]. SYM-H did not return to quiet levels until after June 2. The AE index also shows enhancements exceeding 500 nT throughout most of the period and reinforces that the abnormal drifts seen by the MP ISR can be associated with disturbance electric fields (SQ2).**

- The relative contribution from prompt penetration and disturbed dynamo electric fields is difficult to determine [Fejer and Scherliess, 1997] and is outside the scope of this current presentation.

6. MAIN FINDINGS

- Analyses of 2 years of AMISR-14 2D observations showed that ~50% of isolated post-midnight ESF events occurred locally, that is, within 200 km of JRO.
- Of a total of 27 isolated local events, 60% occurred during geomagnetically disturbed conditions.

➢ **The collocation of AMISR-14 and the Jicamarca ISR allowed us to show, unambiguously, that abnormal upward drifts preceded the development of post-midnight ESF (SQ1).**

➢ **The abnormal drifts were attributed to disturbance electric fields and can contribute, directly, to the linear growth rate of the GRT instability commonly invoked to explain ESF (SQ2).**

- Routine operation of MP ISR and AMISR-14 during the descending phase of solar cycle 25 will allow us to examine, more comprehensively, the drift conditions under which post-midnight ESF develops.

ACKNOWLEDGEMENTS AND REFERENCES

This work was supported by NSF award AGS-2215567 and by the DoD through an NDSEG Fellowship. AAM would like to thank support by UTD through Eugene McDermott Graduate Fellowship 202307. Jicamarca is a facility of the Instituto Geofísico del Perú operated with support from NSF award AGS-2213849 through Cornell University. Geomagnetic indices provided by GFZ Helmholtz Centre and OMNIWeb service.

Gonzalez, W. D. et al. (1994), JGR SP, 99.
Sultan, P. J. (1996), JGR SP, 101.
Fejer, B. G. and Scherliess, L. (1997), JGR SP, 102.
Fejer, B. G. et al. (1999), JGR SP, 96.
Scherliess L. and Fejer, B. G. (1999), JGR SP, 104.
Yizengaw, E. et al. (2013), GRL, 40.
Zhan, W. et al. (2018), GRL, 45.
Rodrigues, F. S. et al. (2023), EPS, 75.
Huba, J. D. (2023), FASS, 4.
Kuyeng, K. et al., in 2023 CEDAR workshop.